Thermally induced changes in the optical properties of SiN x : H films deposited by the electron cyclotron resonance plasma method

F. L. Martnez, A. del Prado, I. Mártil, G. González-Daz, B. Selle, and I. Sieber

Citation: Journal of Applied Physics **86**, 2055 (1999); doi: 10.1063/1.371008
View online: http://dx.doi.org/10.1063/1.371008
View Table of Contents: http://scitation.aip.org/content/aip/journal/jap/86/4?ver=pdfcov
Published by the AIP Publishing

Thermally induced changes in the optical properties of SiN_x:H films deposited by the electron cyclotron resonance plasma method

F. L. Martínez, A. del Prado, I. Mártil,[a] and G. González-Díaz
Departamento de Física Aplicada III, Facultad de Ciencias Físicas, Universidad Complutense de Madrid, E-28040 Madrid, Spain

B. Selle and I. Sieber
Hahn-Meitner-Institut Berlin GmbH, Abteilung Photovoltaik, Rudower Chausse 5, D-12489 Berlin, Germany

(Received 25 February 1999; accepted for publication 17 May 1999)

We analyze the effect of thermal processes on the optical properties (refractive index, optical gap, Tauc coefficient, and Urbach energy) of SiN_x:H films. Films with three different nitrogen to silicon ratios ($x=0.97$, $x=1.43$, and $x=1.55$, respectively) were deposited by a chemical vapor deposition technique assisted by an electron cyclotron resonance generated plasma. After deposition they were subjected to rapid thermal annealing at temperatures ranging from 300 °C to 1050 °C. We found that the percolation threshold for Si–Si bonds (at $x=1.1$) separates films with different response to thermal treatments. The changes of the Tauc coefficient and the Urbach energy at moderate annealing temperatures indicate a structural relaxation of the network for the films with x above the percolation threshold, while at higher temperatures the trends are inverted. In the case of x below the percolation limit the inversion point is not observed. These trends are well correlated with the width of the Si–N infrared stretching absorption band. Additionally the samples with as-grown $x=1.43$ show a good correlation between the Urbach energy and the density of unpaired spins in silicon dangling bonds. © *1999 American Institute of Physics.* [S0021-8979(99)08016-0]

I. INTRODUCTION

Amorphous silicon nitride (a-SiN_x:H) is important from both a fundamental and a technological point of view. Fairly extensive literature has been published about its optical properties,[1] bonding configuration,[2,3] electronic structure,[4,5] and about their applications as active components in thin film transistors[6] (TFTs) and as gate dielectric in metal–insulator–semiconductor field effect transistors (MISFETs).[7,8]

It is well known that amorphous silicon alloys deposited by plasma assisted processes have a high amount of hydrogen incorporated in the network together with nonbonded hydrogen.[9,10] Depending on the application the presence of hydrogen can be beneficial or not. In the case of the TFTs hydrogen is beneficial because the alloy composition that results has approximately the same average number of bonds per atom and bonding constraints per atom as thin film SiO_2,[11] forming a continuous random network with a low density of defects that accounts for optimized TFT performance. On the other hand, for the gate dielectric application in field effect transistors the bonded hydrogen in Si–H and SiN–H arrangements is in part responsible for the inferior electrical performance and device instabilities of low temperature plasma-deposited films relative to nitrides produced by thermal chemical vapor deposition at higher temperatures.[12] The reduction of bonded hydrogen is important for attaining improved electrical properties of a-SiN_x:H films if they are to be used in FET devices because H-atoms and in particular N–H bonding arrangements can serve as precursor sites for defect generation either during the post-deposition device processing or during device operation via current or voltage stress.[13] Although H atoms can passivate silicon dangling bonds and therefore act to decrease the level of interface and bulk trapping states, they can also participate in weak electrostatic H-bonds which are components of a precursor site for charge trapping reactions that can lead to defect generation. Near-neighbor Si–H and SiN–H groups linked through the H-bonding interaction easily trap thermally or optically generated holes that will produce a metastable defect pair.[14]

A postdeposition rapid thermal anneal (RTA) may have different effects on the films depending mainly on the hydrogen content. Moderate annealing temperatures can provide the activation energy necessary to promote the passivation of defects by the formation of Si–H and N–H bonds together with a general relaxation of bonding constraints and stress, and hence produce an improvement in device performance.[15] Higher annealing temperatures may cause hydrogen or nitrogen release. If the evolution of hydrogen brings about Si–N bond healing then the device may improve its characteristics.[16] If, on the contrary, the release of hydrogen leaves unpassivated defects or causes a loss of nitrogen atoms, then a degradation of the performance is observed.[15]

A convenient way of studying the effects of the RTAs on the SiN_x:H is to analyze the changes that these processes induce in their optical properties, particularly in the parameters related to the order or disorder of the network (Tauc slope, Urbach tail, and band gap). In the published literature

[a]Author to whom correspondence should be addressed. Electronic mail: imartil@eucmax.sim.ucm.es

there are few studies about the influence of thermal annealing on the optical properties of SiN_x:H.[17,18] In this article we will focus on the optical properties of SiN_x:H deposited by electron cyclotron resonance (ECR) and subjected to RTA at different temperatures ranging from 300 °C to 1050 °C during 30 s. Films with three different as-grown compositions are considered: $x=0.97$, $x=1.43$, and $x=1.55$. In order to obtain complementary information about the thermal behavior of these films we also studied the N to Si ratio and the infrared spectra. It will be shown that the thermal stability of the films depends on starting compositions above and below the percolation threshold for the Si–Si bonds.

II. EXPERIMENTAL PROCEDURE

We deposited SiN_x:H thin films using an ECR-CVD reactor model ASTEX4500 attached to a high vacuum chamber pumped by a turbomolecular pump. The precursor gases were N_2, which was introduced in the resonance region where the plasma is formed, and SiH_4, which was injected downstream through a gas dispersal ring. We used silica substrates for the optical measurements of transmission and reflection because it is transparent to the ultraviolet light in the range required to characterize the SiN_x:H film. For the composition and other characterizations we used high resistivity (111) *p*-type silicon polished on both sides. The cleaning of the substrates was done using standard chemical procedures starting with dips in acetone and methanol which were followed by drying with nitrogen. This step was common to both types of substrates. Then the wafers were successively subjected to the following cleaning steps: NH_4OH:H_2O_2:H_2O (1:2:5) for 5 min, deionized H_2O, HF:H_2O (1:10) for 1 min and deionized H_2O. Finally the substrates were again blown dry with nitrogen. Immediately afterwards they were introduced in the vacuum chamber, which was pumped down to about 3×10^{-7} mbar before initiating the deposition process. The films were grown without intentional heating, although the plasma raised the temperature of the substrate up to around 60 °C. Several films were grown in the same deposition run and were subsequently subjected to RTA at temperatures ranging from 300 °C to 1050 °C for 30 s. A flow of an inert gas (argon) was maintained during the RTA cycle.

The deposition parameter that strongly influences the composition of the films is the N_2 to SiH_4 gas flow-rate (R), which in this study was selected to produce films with three different compositions. Each of these compositions resulted in films with different characteristic properties that we will explain in the following sections. The nitrogen to silicon ratio (x) of the films was determined by Rutherford backscattering spectrometry (RBS) and energy dispersive x-ray analysis (EDX). RBS spectra were measured with 1.4 MeV He^+ ions and then fitted by the iterative computer program RUBSODY.[19] The given error limits refer only to the statistical error which results from a sequence of eight simulation fits. The EDX analysis was performed with a beam voltage of 5 kV and by comparing with a Si_3N_4 standard sample. The EDX spectra were evaluated by using the so-called Proza method[20] including a correction with respect to the limited film thickness. In EDX, the statistical error for the concentration determination was $\pm0.3\%$. We found the same systematic deviation between the N to Si ratio (x) determined by both methods which was observed and discussed in a previous publication.[21] In this study, therefore, we use for x the average of the RBS and the EDX data. The values of x before postdeposition treatment for the three different types of films analyzed here are:[22] $x=0.97\pm0.03$ for the films deposited with $R=1$, $x=1.43\pm0.02$ for $R=1.6$, and $x=1.55\pm0.04$ for those obtained with $R=7.5$.

IR absorption spectra were measured with a Nicolet 5PC FTIR spectrophotometer. The full width at half maximum (FWHM) of the Si–N stretching absorption band is then obtained from these measurements. This parameter is indicative of the amount of disorder in the film because it is a straightforward measure of the range of N–Si–N bond angles.[23]

For the optical analysis we measured the transmittance and reflectance spectra with a Perkin-Elmer Lambda 9 UV-VIS-NIR spectrometer and calculated the refractive index (n) and extinction coefficient (k) by a method based on the work of Tomlin[24] and Hernández[25] which involves reversed equations of transmittance and reflectance as a function of n and k, with the thickness (d) of the film as a parameter and the wavelength (λ) as independent variable. A test value of d is introduced in the equations and the resulting values of n versus λ are fitted to a Cauchy dispersion rule. Then a computer program varies the parameter d until it obtains the best fit of n versus λ. That value of d is taken as the thickness of the sample and the absorption coefficient (α) is calculated from the corresponding values of k as $\alpha=4\pi k/\lambda$. From the data of the absorption coefficient versus energy ($h\nu$) the values of the band gap (E_g) and the Tauc coefficient B are calculated in the region of strong absorption according to the well known Tauc equation:[26]

$$(\alpha h\nu)^{1/2}=B(h\nu-Eg). \tag{1}$$

At lower absorption levels, below the region of the Tauc edge, there is an exponential tail in $\alpha(h\nu)$ which is generally associated with the intrinsic disorder present in an amorphous solid. In this region the absorption coefficient follows the Urbach relation:[27]

$$\alpha(\nu)=\alpha_0 e^{h\nu/E_0}, \tag{2}$$

where E_0 is the Urbach energy. Among several other explanations of the Urbach edge in amorphous solids, it is widely accepted for the case of silicon nitride to discuss the Urbach edge as a consequence of transitions between localized electronic states in the valence band tail and extended states in the conduction band. Therefore E_0 represents the slope of the valence band tail, which reflects the broadening of the two band edge tails in both Si-rich and N-rich alloys.[28]

III. RESULTS

The average $x=$N/Si ratio from RBS and EDX data is plotted in Fig. 1. The film with as-grown composition $x=1.55$ does not experience any significant change of composition with annealing. On the contrary, the films with $x=1.43$ and $x=0.97$ undergo a significant loss of nitrogen for annealing temperatures above 600 °C.

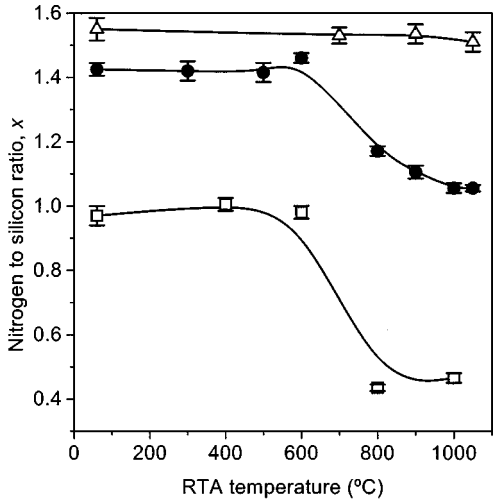

FIG. 1. Average of the nitrogen to silicon ratio obtained from the RBS and EDX measurements as a function of annealing temperature. The as-grown composition of the films are: □ $x=0.97$, ● $x=1.43$, and △ $x=1.55$. Lines are a guide for the eye.

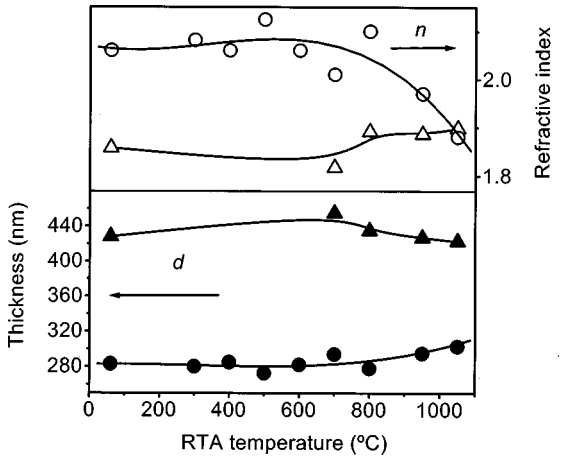

FIG. 3. Lower part: thickness (d) of the films with an as-grown nitrogen to silicon ratio $x=1.43$ (●) and $x=1.55$ (▲) versus annealing temperature. Upper part: refractive index (n) of those two types of films: $x=1.43$ (○) and $x=1.55$ (△) versus annealing temperature. Lines are a guide for the eye.

In Fig. 2 we plot the thickness (d) and the refractive index (n) at a wavelength of 633 nm for the samples with an as-grown composition $x=0.97$. These films experience opposite variations of both parameters with annealing temperature. The increase in the refractive index at higher annealing temperatures may indicate an increase of the density of the polarizable atoms and bonds, or it can also be due to the change in x. As this increase is accompanied by a similar decrease of d, the optical thickness ($n\times d$) remains almost constant. On the contrary, the samples with $x=1.43$ and $x=1.55$ do not show densification on annealing. Their thickness and refractive index are plotted in Fig. 3 as a function of the annealing temperature. In the case of the films with $x=1.55$ both parameters are approximately constant; but in the $x=1.43$ case the results of Fig. 3 indicate a decrease in the refractive index, although d does not significantly change. As the films with as-grown $x=1.43$ loose nitrogen atoms (Fig. 1) for annealing temperatures higher than 600 °C, if their thickness remains constant then the structural density must be smaller, and hence it is consistent that the optical density (which is given by the value of the refractive index) becomes smaller too.

In Fig. 4 we plot the optical gap versus annealing temperature as obtained from the fitting of the experimental data to Eq. (1). The optical gap increases up to a temperature which depends on the composition of the films. The samples with an as-grown composition of $x=1.43$ have the larger increase while the variation is small for those with $x=1.55$ and $x=0.97$. Figures 5 and 6 show the value of the Tauc coefficient and the Urbach slope parameter, respectively. The inverse trends between these two parameters for films with different compositions had been previously observed.[28] Our

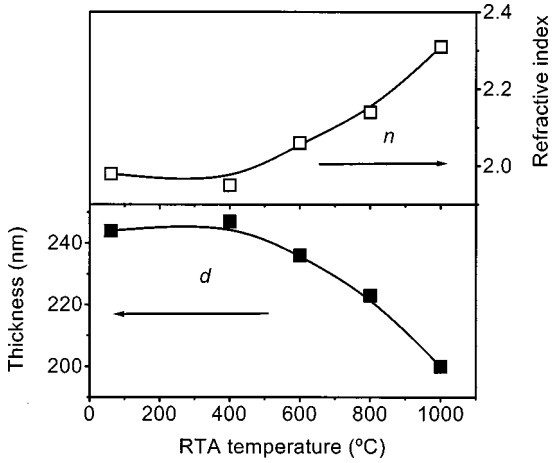

FIG. 2. Thickness (■) and refractive index (□) of the film with an as-grown composition $x=0.97$ versus annealing temperature. Lines are drawn as a guide for the eye.

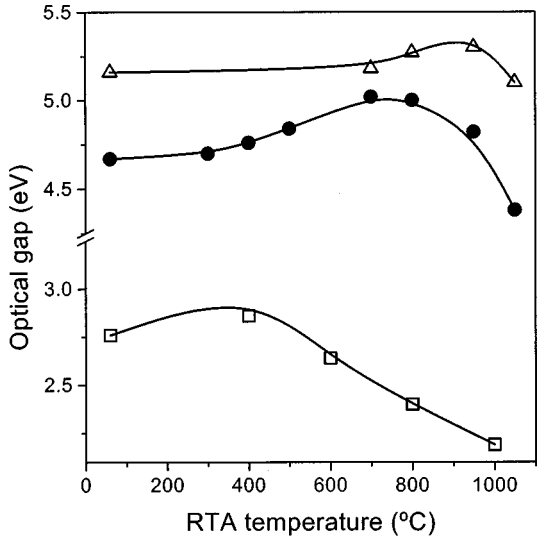

FIG. 4. Optical gap as a function of annealing temperature for the three types of films considered in this study: □ $x=0.97$, ● $x=1.43$, and △ $x=1.55$. The lines are drawn to guide the eye.

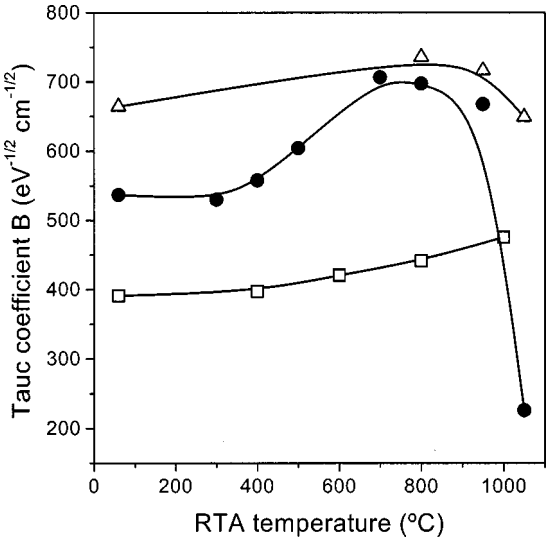

FIG. 5. Tauc coefficient versus temperature of annealing for the films with as-grown composition □ $x=0.97$, ● $x=1.43$, and △ $x=1.55$. The lines are guides for the eye.

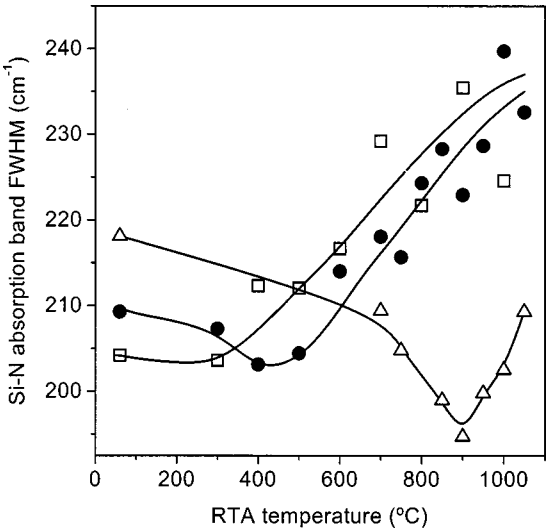

FIG. 7. Full width at half maximum of the Si–N stretching absorption band obtained from the infrared spectra of the films having as-grown compositions □ $x=0.97$, ● $x=1.43$, and △ $x=1.55$. Lines are a guide for the eye.

measurements confirm this opposite correlation of B and E_0 also for films having experienced structural changes induced by RTA.

Figure 7 shows the Si–N stretching band full width at half maximum (FWHM) obtained from the infrared spectra of the films. This parameter is indicative of the amount of disorder in the network because the range of vibration frequencies depends on the distribution of bond angles.[23]

IV. DISCUSSION

In a previous publication[22] we have discussed in detail the physics that explains the results of Fig. 1, so here we will only give a summary. Films with as-grown composition $x=0.97$ and 1.43 lose nitrogen at annealing temperatures above 600 °C while films with an as-grown nitrogen to silicon ratio of $x=1.55$ maintain a constant composition. The explanation of the different behavior of the films with $x=0.97$ and 1.43 with respect to those with $x=1.55$ is related to the different ways in which hydrogen is bonded in these samples. Films with as-grown compositions $x\leqslant 1.43$ show the presence of both Si–H and N–H bonds. Si–H bonds are predominant in the samples with $x=0.97$ and N–H bonds predominate in those with $x=1.43$. At annealing temperatures below 600 °C, N–H bonds are replaced by Si–H ones according to the well known network interchange reaction proposed by Yin and Smith:[29]

$$\text{Si–Si}+\text{N–H}\rightarrow\text{Si–N}+\text{Si–H}. \tag{3}$$

At annealing temperatures above 600 °C these films lose both hydrogen and nitrogen through a collective process that involves all bonds present in the network:

$$\text{Si–H}+\text{H–NSi–H}\rightarrow\text{Si–Si}+\text{NH}_3\uparrow. \tag{4}$$

By contrast, in the films with $x=1.55$ hydrogen is only fixed to N–H bonds and no Si–H bonds are observed in the IR spectrum. Therefore this reaction cannot take place and the release of hydrogen at high temperatures does not cause a loss of nitrogen. In this case it has been proposed[12,30] that the reaction that takes place is the following:

$$\text{Si–N–H}+\text{Si–N–H}\rightarrow 2(\text{Si–N})+\text{H}_2\uparrow. \tag{5}$$

The values of refractive index and thickness plotted in Fig. 2 indicate that in the case of the sample with $x=0.97$ there is a well-defined trend of densification with increasing annealing temperature. These parameters behave quite differently for the films with $x=1.43$ and $x=1.55$, where the thickness remains constant and the refraction index for the $x=1.43$ case decreases at high annealing temperatures. There are several published results relating composition and refractive index.[31] Knolle[32] finds a linear correlation between n and the atomic percent of Si, while Makino[33] reported that the refractive index of nonstoichiometric SiN_x:H films can be represented as the bond density weighted linear combina-

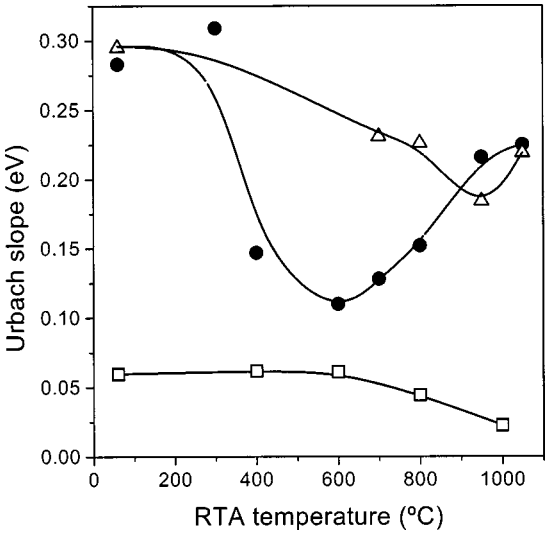

FIG. 6. Urbach energy as a function of RTA temperature for the films analyzed in the text: □ $x=0.97$, ● $x=1.43$, and △ $x=1.55$. The lines are drawn as a guide for the eye.

tion of the refractive indices of a-Si:H and a-Si_3N_4. Evaluating our data by this model we have found a good coincidence between measured and calculated values for the as-grown samples. However, the calculated values of n for the RTA treated films move towards the value of amorphous silicon ($n=3.3$) when there is a loss of nitrogen produced by the RTA (films with as-grown $x=1.43$ and $x=0.97$), while the measured values do not show this shift for the films with $x=1.43$. A qualitative correlation between optical and structural density can be realized by a comparison of the optical refraction index n with the packing density resulting from the quantity $N\times d$ determined by RBS, where N is the total atomic density including Si and N atoms (but not H atoms which cannot be detected by the RBS), although it must be observed that differences in x may have effects in the bonding configuration (proportion of Si–Si and Si–N bonds), and therefore in the refractive index, that are not considered in this correlation. The ratio of the film density to the bulk density is called the packing density, where the film atomic density (N_{film}) is determined comparing the thickness values with the RBS area density ($N\times d$), while the bulk density (N_{bulk}) can be estimated by a linear interpolation (extrapolation) between the bulk densities of silicon and of stoichiometric silicon nitride assuming that the compound SiN_x is free of hydrogen. For the experimental values of x in excess of 4/3 one gets $N_{\text{bulk}}>N(Si_3N_4)$ and hence the presence of hydrogen which has not been taken into account is indicated indirectly. We calculated the packing density by this procedure and we found that the trends are analogous to the calculated n, although the values of the packing density were systematically lower due to the effect of ignoring the hydrogen content. It seems therefore that the refractive index obtained from the transmittance and reflectance spectra by the method outlined in the experimental section is not sensitive to the change of composition caused by the thermal release of nitrogen. Nevertheless, further evidence is needed to confirm this conclusion, given the influence that a change in the relative densities of Si–Si and Si–N bonds may have in n. Because the increase of n with annealing temperature for the films with $x=0.97$ is lower than what would be expected by the loss of nitrogen, it is more likely to cause the decrease of thickness that it is observed for these films. No change of thickness is detected for the films with $x=1.43$, even though they lose nitrogen in an analogous way as the films with $x=0.97$. The films with $x=0.97$ and $x=1.43$ differ in the point that $x=0.97$ is below the percolation threshold[28] ($x=1.1$) of Si–Si bonds in the lattice of the nitride while $x=1.43$ is above that limit. The continuous chains of Si–Si bonds that spans throughout the whole network for compositions below the percolation threshold may contribute to facilitate the densification observed for the $x=0.97$ films. No percolation occurs for $x=1.43$ and 1.55 and these films do not experience densification.

The results for the optical gap plotted in Fig. 4 are explained by the same Eqs. (3) and (4) as the process of hydrogen redistribution and release for the samples with $x=0.97$ and $x=1.43$. The initial increase of the optical gap with low annealing temperatures is due to the substitution of Si–Si bonds by Si–H bonds because Si–H σ states lie deeper than Si–Si σ states, thereby lowering the valence band edge E_v, while Si–H σ^* states lie at a similar energy as Si–Si σ^* states so that the conduction band energy E_c is little changed.[4] The same argument in the opposite sense explains why the process of hydrogen and nitrogen release given by Eq. (4) produces a decrease of the optical gap. In this case we assume the formation of Si–Si bonds and the breaking of Si–H bonds, together with the release of nitrogen, and it is well known[4] that changes in composition in the range $1.1<x<1.4$ have a strong influence on E_g.

The network bond reactions, Eqs. (3) and (4), are not valid for the samples with $x=1.55$ because they only have N–H bonds and not Si–H bonds. Above 900 °C we observe a decrease of the optical gap accompanied by a significant loss of N–H bonds from $2.5\times10^{22}\,\text{cm}^{-3}$ at 900 °C to $1.2\times10^{22}\,\text{cm}^{-3}$ at 1050 °C as it was described by Eq. (5). According to Robertson[4] the reason for this behavior is that in a-SiN_x:H the introduction of $=$NH groups widens the gap by raising E_c. E_v is not lowered because the valence-band maximum is still formed by Npπ states. The raising of E_c appears to be due to an admixture of N–H states, which have a wider gap. Therefore this explains the reduction of the optical gap when the N–H bonds are lost in the samples with $x=1.55$.

There is a remarkable coincidence in the trends observed for the Tauc coefficient B and the Urbach slope parameter E_0 shown in Figs. 5 and 6, respectively. These two parameters are indicative of the degree of tailing at the band edges. B is the slope of the fit of Eq. (1) used to determine the optical gap and E_0 is the inverse slope of the lower exponential part of the optical absorption edge and reflects the slope of the valence-band tail, which is broader than the conduction-band tail in both Si-rich and N-rich alloys. According to the results pointed out by Robertson[28] the clustering that occurs around the percolation threshold $x=1.1$ produces a strong tailing of band edges: this causes a minimum in the Tauc slope at around $x=1.0$ and a maximum in the Urbach energy E_0 at around $x=1.4$ in agreement with the trends that we obtained for these parameters for the as-grown compositions $x=0.97$, 1.43, and 1.55. Regarding the dependence on the annealing temperature we observe two different behaviors[34] depending on whether the as-grown composition is above or below the percolation limit $x=1.1$. The samples with $x=1.43$ and 1.55 show a change of E_0 and B with annealing temperature that is controlled[28] by the diffusion of hydrogen in a-SiN_x:H. Hydrogen is the most mobile atom in both a-SiN_x:H and a-Si:H and thus is generally considered to be responsible for structural changes which occur below the crystallization temperature. When the deposition is carried out at room temperature the diffusion coefficient of hydrogen in a-SiN_x:H is so small that every hydrogen atom will remain at that bonding site which it has occupied at the end of the deposition process. Thus the structure of the deposited a-SiN_x:H film is metastable and essentially determined by an effective temperature characteristic for the glow-discharge plasma used for the film deposition. When the films are annealed at temperatures below 600 °C for the samples with $x=1.43$, and below 950 °C for the samples with $x=1.55$ the network undergoes relaxation and recon-

struction which is observed as an increase of B and a decrease of E_0 and also as an increase of the optical gap mentioned before. In the range of these temperatures there is no release of hydrogen and in the case of the sample with $x=1.43$ we have observed from the infrared spectra of the films[22] that the nonbonded hydrogen trapped in microvoids of the structure forms bonds with the atoms of the lattice, increasing the density of Si–H bonds from $4\times10^{21}\,\mathrm{cm}^{-3}$ for the nonannealed sample to about $7\times10^{21}\,\mathrm{cm}^{-3}$ for the sample annealed at 600 °C, therefore saturating defects and making the increase of order more pronounced than for the samples with $x=1.55$. Under temperatures above 700 °C for $x=1.43$ and 950 °C for $x=1.55$, respectively, the diffusion coefficient for hydrogen is so large that most of the hydrogen will leave the a-SiN_x:H sample during the annealing. In this case, E_0 will increase and B will decrease, because the reconstruction process has increasingly to be carried out by the much slower movement of Si and N atoms. This behavior is in agreement with the trends of Figs. 5 and 6. Additionally, for the samples with as-grown $x=1.43$ another effect, superimposed to the release of hydrogen, is the loss of nitrogen which takes place at temperatures above 600 °C. Due to this loss of nitrogen the composition of the sample changes from around $x=1.4$ at annealing temperatures below 600 °C to $x=1.055$ at 1050 °C, that is to say, the composition moves towards the percolation limit $x=1.1$ in this range of temperatures. As the strongest tailing of band edges may be produced around the percolation threshold, this effect enhances the decrease in B and the increase in E_0 for these samples with respect to those with $x=1.55$ which do not experience any change of composition. In the case of E_0 this would mean that its maximum value would be around $x=1.1$ when the changes of composition are induced by annealing, rather than 1.4 as it was found by Robertson[28] comparing data with different compositions obtained with different growth parameters from several authors.

The case of the sample $x=0.97$, whose as-grown composition is below the percolation threshold, is different. Both B and E_0 remain almost constant with annealing temperature, with a monotonical and slight increase of B and a similar decrease of E_0. We have already noted this different behavior of the film with $x=0.97$ with respect to the others in the refractive index and thickness. It seems clear that the percolation threshold separates into two types of films with different structural properties. Below $x=1.1$ there is a percolation of the Si–Si bonds in the lattice and it is known that the sp^3 hybridization of the silicon atoms forms a tetrahedron which is a very rigid structure. When the silicon proportion is increased, that is, x falls below the percolation threshold, the connectivity of the covalent bonds is enhanced because of the high coordination number $(=4)$ of silicon, producing a structure which is much more rigid and stressed. As a consequence, the films with $x=0.97$ remain almost unaffected by the thermal relaxation, as shown in Figs. 5 and 6. Additionally, these films have very few N–H bonds, and it is well-known[35] that a low content of [NH] leads to an increase in stress because the absence of the N–H bonds reduces the flexibility of the SiN_x:H network.

Figure 7 shows another parameter which is indicative of the disorder in the network: the width of the Si–N absorption band. A wider band indicates a higher disorder. The dependence of this parameter with annealing temperature for the films with $x=1.43$ and 1.55 takes the U-shaped form similar to those of the Urbach slope parameter, indicating an initial increase of order at low annealing temperatures and a subsequent increase of disorder at high temperatures. The only difference with respect to E_0 is that the minimum value of the curve occurs at lower temperatures: 900 °C for the films with as-grown $x=1.55$ (instead of 950 °C) and 400 °C for the films with $x=1.43$ (instead of 600 °C). These differences in the optimum temperatures can be understood in terms of the different stress of the films due to the different substrates used for the measurements (silicon for the IR spectra and silica for the optical properties). The samples with $x=0.97$ have again a different behavior, showing no initial decrease of FWHM and an important increase above 300 °C. The FWHM shows that the strain of these structures is not relaxed by the RTA, corresponding to the changes in B and E_0 parameters,

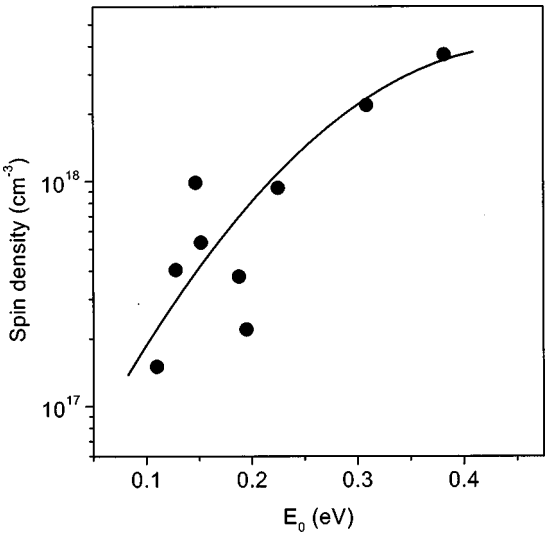

FIG. 8. Density of unpaired spins in silicon dangling bonds as a function of the Urbach slope parameter E_0 for the films with as-grown nitrogen to silicon ratio of $x=1.43$. The line is a guide for the eye.

Finally, we show in Fig. 8 some preliminary results of the dangling bond density measured by electron spin resonance (ESR) versus the Urbach slope coefficient for the samples with the lower content of total bonded hydrogen (the films with as-grown $x=1.43$). The trend observed for this sample series reproduces quite well the general trend found by Stutzmann[36] in amorphous hydrogenated silicon, in which he proposed his weak bond-dangling bond conversion model. According to the Stutzmann's model the behavior of the dangling bond density with temperature must be parallel to that of E_0 because of the structural transformation between weak bonds and dangling bonds.

V. CONCLUSIONS

We have described the optical properties of a-SiN_x:H films which have been subjected to rapid thermal annealing, and we have related them with the changes in composition,

hydrogen content, and structural disorder. The index of refraction and thickness experience opposite variations for the samples with an as-grown composition below the percolation threshold of Si–Si bonds. The as-grown values of n agree with predicted values based on composition considerations, but it was not possible to relate the thermal behavior of n with changes in composition. The optical gap increases at low annealing temperatures as a consequence of hydrogen redistribution and structure relaxation. Above a certain temperature, which depends on the composition, the optical gap decreases due to the loss of hydrogen, and for the films with both Si–H and N–H bonds also because of the loss of nitrogen. The variation of the optical parameters that account for the disorder in the film (Urbach slope and Tauc coefficient) is different depending on whether the composition is above or below the percolation limit of Si–Si bonds in the matrix of silicon nitride. Above the percolation limit there is an initial increase of order followed by a decrease at higher annealing temperatures. Below the percolation limit only a slight and monotonical variation is detected along with a compaction of the film. This different behavior is interpreted as a consequence of the higher stress occurring in the films with a nitrogen to silicon ratio below the percolation limit. Preliminary measurements of the density of silicon dangling bonds enabled us to compare this parameter with the Urbach tail slope, verifying the weak bond/dangling bond conversion model, proposed by Stutzmann, for the case of the films with a lower density of total bonded hydrogen.

ACKNOWLEDGMENTS

The authors are indebted to Dr. J. Cárabe and Dr. J. Gandía from the National Center for Energy Research (CIEMAT) for the use of the spectrometer facility, licensing of their useful software GRAFO for optical analysis, and many helpful discussions. Their friendship and support are greatly appreciated, as well as those of the technical center CAI Implantación Iónica of the University of Madrid and the financing from the Science Ministry of Spain under contract TIC98-0740.

[1] E. A. Davis, N. Piggins, and S. C. Bayliss, J. Phys. C **20**, 4415 (1987).
[2] S. Hasegawa, M. Matsuda, and Y. Kurata, Appl. Phys. Lett. **58**, 741 (1991).
[3] S. García, J. M. Martín, M. Fernández, I. Mártil, and G. González-Díaz, Philos. Mag. B **73**, 487 (1996).
[4] J. Robertson, Philos. Mag. B **63**, 47 (1991).
[5] W. L. Warren, J. Kanicki, F. C. Rong, and E. H. Poindexter, J. Electrochem. Soc. **139**, 880 (1992).
[6] S. S. He, M. J. Williams, D. J. Stephens, and G. Lucovsky, J. Non-Cryst. Solids **164-166**, 731 (1993).
[7] D. G. Park, Z. Chen, A. E. Botchkarev, S. N. Mohammad, and H. Morkoç, Philos. Mag. B **74**, 219 (1996).
[8] C. G. Parker, G. Lucovsky, and J. R. Hauser, IEEE Electron Device Lett. **19**, 106 (1998).
[9] H. J. Stein, S. M. Myers, and D. M. Follstaedt, J. Appl. Phys. **73**, 2755 (1993).
[10] R. E. Norberg, D. J. Leopold, and P. A. Fedders, J. Non-Cryst. Solids **227-230**, 124 (1998).
[11] G. Lucovsky and J. C. Phillips, J. Non-Cryst. Solids **227-230**, 1221 (1998).
[12] Z. Lu, P. Santos-Filho, G. Stevens, M. J. Williams, and G. Lucovsky, J. Vac. Sci. Technol. A **13**, 607 (1995).
[13] Z. Jing, G. Lucovsky, and J. L. Whitten, J. Vac. Sci. Technol. B **13**, 1613 (1995).
[14] Z. Lu, S. S. He, Y. Ma, and G. Lucovsky, J. Non-Cryst. Solids **187**, 340 (1995).
[15] D. G. Park, Z. Chen, D. M. Diatezua, Z. Wang, A. Rockett, H. Morkoç, and S. A. Alterovitz, Appl. Phys. Lett. **70**, 1263 (1997).
[16] Y. Ma, T. Yasuda, and G. Lucovsky, J. Vac. Sci. Technol. A **11**, 952 (1993).
[17] K. C. Lin and S. C. Lee, J. Appl. Phys. **72**, 5474 (1992).
[18] L. Cai, A. Rohatgi, D. Yang, and M. A. El-Sayed, J. Appl. Phys. **80**, 5384 (1996).
[19] A. Witzman, RUBSODY Users Guide, Friedrich-Schiller-Universität, Jena, 1992.
[20] G. F. Bastin and H. J. M. Heijligers, Scanning **12**, 225 (1990).
[21] I. Sieber, A. Schoepke, and B. Selle, Fresenius J. Anal. Chem. **353**, 639 (1995).
[22] F. L. Martínez, I. Mártil, G. González-Díaz, B. Selle, and I. Sieber, J. Non-Cryst. Solids **227-230**, 523 (1998).
[23] D. V. Tsu, G. Lucovsky, and N. J. Mantini, Phys. Rev. B **33**, 7069, (1986).
[24] S. G. Tomlin, J. Phys. D **1**, 1667 (1968).
[25] J. L. Hernández-Rojas, M. L. Lucía, I. Mártil, G. González-Díaz, J. Santamaría, and F. Sánchez-Quesada, Appl. Opt. **31**, 1606 (1992).
[26] J. Tauc, R. Grigorovici, and A. Vancu, Phys. Status Solidi **15**, 627 (1966).
[27] R. Urbach, Phys. Rev. **92**, 1324 (1953).
[28] J. Robertson, Philos. Mag. B **69**, 307 (1994).
[29] Z. Yin and F. W. Smith, Phys. Rev. B **43**, 4507 (1991).
[30] F. L. Martínez, A. del Prado, D. Bravo, F. López, I. Mártil, and G. González-Díaz, J. Vac. Sci. Technol. A **17**, 1280 (1999).
[31] S. A. Almeida and S. R. P. Silva, Thin Solid Films **311**, 133 (1997).
[32] W. R. Knolle, Thin Solid Films **168**, 123 (1989).
[33] T. Makino, J. Electrochem. Soc. **130**, 450 (1983).
[34] F. L. Martínez, I. Mártil, G. González-Díaz, A. M. Bernal-Oliva, J. M. González-Leal, and E. Márquez, Thin Solid Films **343-344**, 428 (1999).
[35] S. Hasegawa, Y. Amano, T. Inokuma, and Y. Kurata, J. Appl. Phys. **72**, 5676 (1992).
[36] M. Stutzmann, Philos. Mag. B **60**, 531 (1989).